

Two-Dimensional Electronic Spectroscopy Reveals Ultrafast Energy Diffusion in Chlorosomes

Jakub Dostál,^{†,‡} Tomáš Mančal,[‡] Ramūnas Augulis,^{†,||} František Vácha,[§] Jakub Pšenčík,[‡] and Donatas Zigmantas^{*,†}

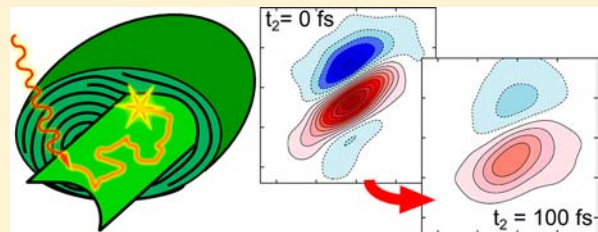
[†]Department of Chemical Physics, Lund University, Getingevägen 60, 221 00 Lund, Sweden

[‡]Faculty of Mathematics and Physics, Charles University in Prague, Ke Karlovu 3, 121 16 Prague, Czech Republic

[§]Faculty of Science, University of South Bohemia, Branišovská 31, 370 05 České Budějovice, Czech Republic

Supporting Information

ABSTRACT: Chlorosomes are light-harvesting antennae that enable exceptionally efficient light energy capture and excitation transfer. They are found in certain photosynthetic bacteria, some of which live in extremely low-light environments. In this work, chlorosomes from the green sulfur bacterium *Chlorobaculum tepidum* were studied by coherent electronic two-dimensional (2D) spectroscopy. Previously uncharacterized ultrafast energy transfer dynamics were followed, appearing as evolution of the 2D spectral line-shape during the first 200 fs after excitation. Observed initial energy flow through the chlorosome is well explained by effective exciton diffusion on a sub-100 fs time scale, which assures efficiency and robustness of the process. The ultrafast incoherent diffusion-like behavior of the excitons points to a disordered energy landscape in the chlorosome, which leads to a rapid loss of excitonic coherences between its structural subunits. This disorder prevents observation of excitonic coherences in the experimental data and implies that the chlorosome as a whole does not function as a coherent light-harvester.



INTRODUCTION

Photosynthetic organisms developed various types of light-harvesting antennae to efficiently collect incoming sunlight. Generally, these are sophisticated protein complexes where pigments are held in appropriate positions by a protein scaffold. The only known exception to this molecular architecture is the chlorosome, an extraordinary large light-harvesting antenna found in three phyla of photosynthetic bacteria.^{1–3} The chlorosome interior is composed of up to a few hundreds of thousands of strongly interacting bacteriochlorophyll (BChl) *c*, *d*, or *e* molecules self-assembled into aggregates without any direct involvement of a protein. This unique composition allows mimicking the chlorosomes by aggregates of chlorosomal BChls or their synthetic analogues prepared in vitro, which could be potentially utilized in, for example, artificial photosynthesis or photovoltaics.^{4–8} Experiments employing X-ray scattering and electron cryomicroscopy revealed that BChl aggregates are organized into curved lamellar structures^{9–12} ranging from disordered lamellae prevailing inside the wild-type chlorosomes, to well-organized multilayered cylinders observed mainly for a specific bchQRU mutant of *Chlorobaculum (Cba.) tepidum*.^{10,12} However, the overall organization of BChl aggregates in each chlorosome is unique, and it exhibits a significant variability even inside a single chlorosome. This prevents the structure of the aggregates from being determined at the molecular level by X-ray crystallography. The exact arrangement of BChls within the chlorosome is therefore still a matter of dispute. Several models of

the short-range organization have been proposed, mainly based on NMR experiments.^{13–17}

Fast photophysical processes in chlorosomes were studied by several groups (for reviews, see refs 3,12). It was observed that excitation of the Q_y band of BChl aggregates is followed by a rapid exciton relaxation, which is finished in less than 1 ps.^{18–20} This process is followed by long-range energy transfer within the aggregates leading to excitation equilibration over the whole chlorosome.¹⁹ From BChl aggregates, the excitation energy is transferred to BChl *a* molecules in the baseplate, a pigment–protein complex located on the side of the chlorosome facing the cytoplasmic membrane. This step occurs on the time scale of tens of picoseconds, depending on the type of aggregated BChls.²¹ Subsequently, the excitation is transferred toward the reaction centers in the cytoplasmic membrane, where charge separation occurs. In addition to relaxation processes, coherent oscillations were also observed and attributed to intramolecular vibrational wavepacket dynamics.^{22–26}

To get a deeper insight into photophysical processes in chlorosomes, we have employed electronic two-dimensional (2D) spectroscopy.²⁷ The real part of the 2D spectrum can be interpreted as a spectrally resolved transient spectrum mapped on the two frequency axes, where ω_1 is the excitation frequency, ω_3 is the detection frequency, and t_2 is the system evolution

Received: March 16, 2012

Published: June 12, 2012



time. It has been demonstrated that 2D spectroscopy, apart from revealing energy transfer dynamics, has enabled observation of coherent electronic dynamics in small photosynthetic complexes,^{28,29} and supplied means for tracking dynamic line shape changes due to electron–phonon interactions.^{30–32} The 2D line shapes thus provide information on the spectral changes even within the homogeneous line width that are not accessible from pump–probe experiments. The limitations of the pump–probe spectra are due to the fact that they are related to 2D spectra by integration along the excitation (ω_1) axis.²⁷ One example of information that is lost by this integration is the pure dephasing process. This results in change of the observable 2D line shape, while the corresponding pump–probe spectrum remains unaltered.

This work explores initial dynamics (up to 200 fs after excitation) at ambient temperature within chlorosomes containing BChl *c* from green sulfur bacterium *Cba. tepidum*. The extra dimension of coherent 2D spectroscopy and high simultaneous spectral and time resolution have enhanced the information content of ultrafast experiments. Excitation energy dynamics have been unraveled in chlorosomes taking place on a sub-100 fs time scale. This is attributed to ultrafast energy migration between different structural units that assures extremely efficient energy flow through a lamellar layer, which is essential to the light-harvesting function of the chlorosome.

■ EXPERIMENTAL RESULTS

The NIR part of the steady-state absorption spectrum of the chlorosome from *Cba. tepidum* is shown in Figure 1. The spectrum

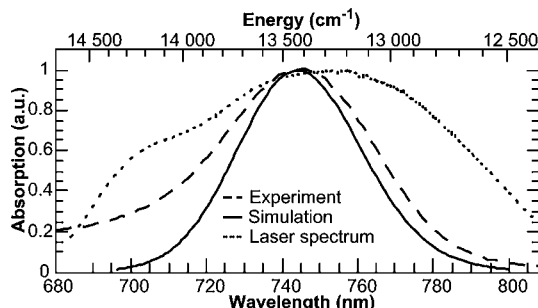


Figure 1. Absorption spectrum of chlorosomes from *Cba. tepidum* (—) and its simulation (—) together with a spectral profile of the laser pulses (···).

is dominated by the Q_y band of aggregated BChl *c* centered at 745 nm with full width at half-maximum (fwhm) of the absorption band corresponding to 930 cm⁻¹. Absorption of BChl *a*-rich baseplate at around 800 nm is negligible because of low abundance of BChls *a* (~1%) in the chlorosome. The spectral profile of the laser pulse completely covering the absorption band is also shown. Figure 2 depicts corresponding 2D spectra (real part of the electric field) measured at population times between 0 and 200 fs. The total spectra composed of rephasing and nonrephasing parts are shown, providing an intuitive picture of emissive/absorptive signals on the map of excitation and probe frequencies. The 2D spectrum measured at 0 fs allows an upper estimate of the homogeneous line width of the exciton transition between the ground and first excited states of BChl *c* aggregate, which is 360 ± 20 cm⁻¹. This value is similar to the estimate of the homogeneous line width used in exciton calculations.²⁶

The 2D spectrum undergoes dramatic changes during this short time period. In the beginning, the signal exhibits a strong positive feature (corresponding to ground-state bleaching and stimulated emission), which is extensively elongated along the diagonal implying

strong correlation of excitation and detection frequencies. The central positive part of the signal is surrounded by negative features due to broad excited-state absorption. During the first 100 fs, the amplitude of the positive signal drops significantly and its line shape becomes more rounded, while the negative part at the lower ω_3 frequencies disappears, because of overlap with the broadened positive signal. The amplitude of the signal at the position of its initial maximum drops to approximately one-half with an effective time constant of 40 fs (Figure 3). The overall transient absorption signal, which is obtained by integration of the 2D spectrum along its horizontal (ω_1) axis, evolves rapidly during the first 100 fs, by which time it reaches an almost stationary level (Figure 4). The time evolution of this projection reflects the fast changes of the 2D line shape; however, the exact shape evolution is not captured. Previously reported oscillating dynamics^{22,24–26} were not resolved here due to their low frequency, corresponding to a typical period of ~220 fs (comparable to the time window used here), and due to the low amplitude of the oscillations at room temperature. Qualitatively similar behavior of 2D spectra was also observed for chlorosomes from *Chloroflexus aurantiacus* (see the Supporting Information).

■ MODELING AND DISCUSSION

Role of Disorder. The chlorosome is an aggregate of tightly packed BChls, where the resonant coupling between chromophores is strong and aggregate eigenstates involve excited states of more than one molecule.^{12,19,26} In a perfect large periodic aggregate, strong resonance coupling would result in energy eigenstates delocalized over the whole system. The presence of significant disorder in the aggregate structure results in a certain distribution of transition frequencies (so-called diagonal energetic disorder) and couplings between molecules (off-diagonal disorder). Thus, one may assume that the aggregate consists of a number of domains separated by a high local energetic disorder or by a significant structural dislocation. The wave function of the aggregate's excited states cannot then be fully delocalized over the aggregate, but would remain delocalized only over one domain or only over a part of the domain. Further, in this Article, we refer to these regions as coherent domains. The electronic transitions between the coherent domains would couple only relatively weakly with respect to the electron–phonon coupling, and the energy transfer between them would thus proceed in an incoherent fashion described, for example, by multichromophoric Förster rate theory.^{33,34} The domain picture provides a more intuitive explanation of spectroscopic observations than treating the disordered aggregate as a whole, as we will discuss below. Also, in the situation when it is possible to theoretically treat only the two limiting cases of strong and weak resonance coupling, the partitioning into coherent domains may provide an effective tool for detailed simulations of large aggregates.

Chlorosome Structure. In all current models of chlorosomes, the BChl aggregates are organized in curved lamellar structures that can include multilayered cylinders.^{9–12} The lamellar spacing was determined to be on the order of 2–3 nm.^{9,10} At these distances, weak interactions lead to a negligible delocalization,³⁵ and the energy transfer between the lamellar layers can be described by an incoherent rate theory.^{33,34} Thus, one can view the interior of the chlorosome as an ensemble of layers. The disorder within individual layers prevents delocalization of excitonic eigenstates of the system over the whole two-dimensional structure of the layer. Thus, even one lamellar layer should be viewed as an ensemble of coherent domains. The excitation could move along the two-dimensional structure in both the coherent fashion (e.g., within the coherent

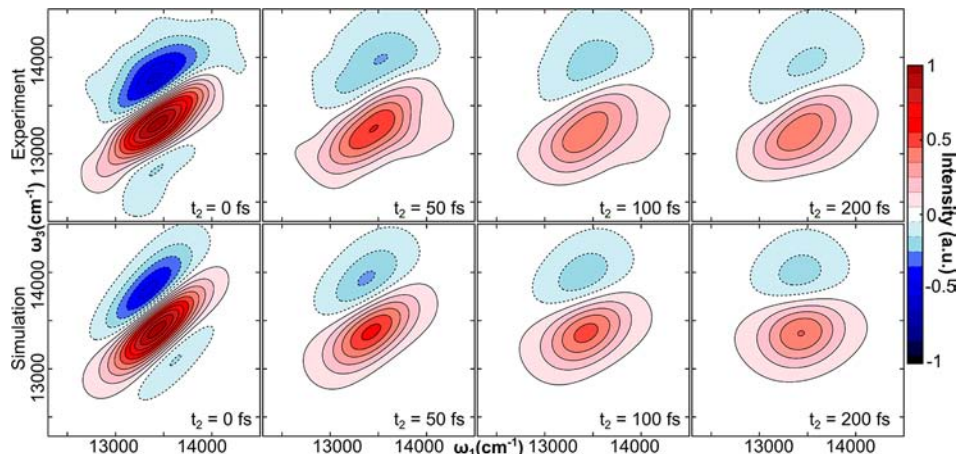


Figure 2. Measured (top) and simulated (bottom) 2D spectra (real part of electric field) of chlorosomes at different population times.

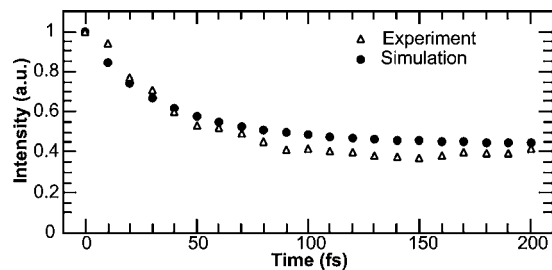


Figure 3. Amplitude decay of the positive peak in experimental (Δ) and simulated (\bullet) 2D spectra at the point of its maximum initial signal.

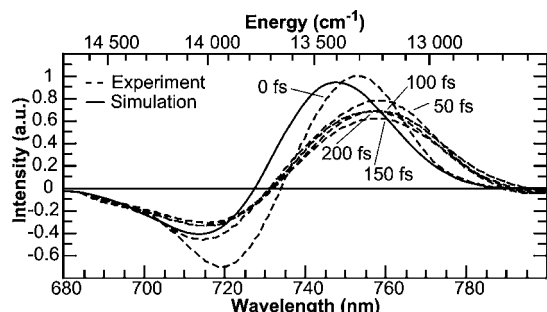


Figure 4. Transient absorption spectra of chlorosomes obtained by integration of 2D spectra along the ω_1 axis. Five different population times (—) and the time invariant simulated curve (—) are shown.

domains) and the incoherent fashion (between the coherent domains).

We face a situation in which measured spectra inevitably contain an averaging over a hierarchy of various types of static disorder. The highest level of disorder includes variations among chlorosomes and among individual lamellar layers within one chlorosome. The distribution associated with this highest level of disorder can be estimated from low temperature spectral hole-burning and fluorescence experiments, which can measure the distribution of the lowest excitonic levels in the ensemble of chlorosomes. The fwhm values in the range of 100–250 cm^{-1} have been determined for chlorosomal aggregates,^{36,37} indicating a relatively small contribution of the highest level of disorder to the broad absorption bands ($\sim 1000 \text{ cm}^{-1}$) of chlorosomes from green sulfur bacteria. Similarly, single molecule spectroscopy, which shows the

variations between individual chlorosomes, revealed that low and ambient temperature fluorescence spectra of single chlorosomes from *Cba. tepidum* do not exhibit significant narrowing as compared to the bulk spectrum.^{38–41} From the above discussion, it can be concluded that the differences among the individual coherent domains are responsible for the broad absorption spectrum of the chlorosome as well as for the elongated shape of 2D correlation spectrum at $t_2 = 0 \text{ fs}$.

Ultrafast Line Shape Dynamics. Unlike linear and some nonlinear (transient) absorption spectroscopies, coherent 2D spectroscopy enables, to a large extent, one to overcome the loss of information due to the static disorder. It is reasonable to assume that the coherent domains in the chlorosome have a distribution of allowed transition frequencies, and that the spectral line shapes corresponding to electronic transitions associated with individual domains are significantly narrower than the ensemble line shape. The 2D spectrum at $t_2 = 0 \text{ fs}$ is expected to have a characteristic elongation along the diagonal. This is exactly what is observed in the experiment. Evolution of the diagonal line shape with $t_2 > 0 \text{ fs}$ then monitors the redistribution of the excitation in and among the domains. At very short times (sub-100 fs), no redistribution is possible on the highest level of structural hierarchy, that is, among the lamellar layers or over the whole chlorosome. The transitions between the layers in the chlorosomes were observed on the time scale of picoseconds.^{19,24,26,37} Fast energy redistribution can, however, be expected within and between the domains in the same 2D lamellar layer, because of the close proximity of coherent domains.

An alternative interpretation of sub-100 fs changes might involve homogeneous line shape dynamics of excitonic transitions due to the interaction with the bath. However, in the following, we will show that this cannot be the case. Let us first estimate the homogeneous line width corresponding to electronic transitions associated with individual coherent domains. This line width has to be compared to the diagonal width of the observed 2D spectrum. To this end, we will assume a line shape function of an individual BChl molecule that has the form of an overdamped Brownian oscillator:⁴²

$$g_{\text{BChl}}(t) = \frac{2\lambda_{\text{BChl}}kT}{\hbar\Lambda^2}(e^{-\Lambda t} + \Lambda t - 1) \approx \frac{1}{2}\Delta^2 t^2 \quad (1)$$

The two parameters of this model are the reorganization energy λ_{BChl} and the bath correlation time τ_c , which enters through the parameter $\Lambda = 1/\tau_c$. For the estimation of the line shape fwhm,

we introduced a short time expansion of the line shape function⁴³ and ignored the imaginary part of the line shape function, which leads only to a frequency shift. We also introduced a line shape parameter $\Delta^2 = 2\lambda_{\text{BChl}}k_B T \hbar^{-1} = C_{\text{BChl}}(0)$, where $C_{\text{BChl}}(t)$ is the energy gap correlation function of the BChl transition. The line shape of an individual electronic transition will be narrowed by exciton interaction, and, at the same time, broadened due to finite lifetime of the exciton. In a sufficiently large system of molecules interacting through nearest neighbor coupling, the line narrowing factor is $\sim 1/N$, where N is the number of interacting molecules in the system. Correspondingly the excitonic line shape would be significantly narrowed.

The reorganization energy of BChl *c* at 300 K can be estimated from the Q_y band's Stokes shift to be in the range 35–90 cm⁻¹ depending on the solvent used.⁴⁴ The corresponding upper estimate of a BChl *c* homogeneous line width in solution is $\sigma_{\text{BChl}} = \Delta(8 \ln 2)^{1/2} = 457 \text{ cm}^{-1}$. The lifetime broadening coming from the excitonic relaxation on the time scale of 100 fs amounts to 53 cm⁻¹, which can be neglected, leaving us with the value of 457 cm⁻¹ as the least favorable upper estimate of homogeneous line width of excitonic levels. However, the actual fwhm of the Q_y band in the *Cba. tepidum* chlorosome is a factor of 2 higher (900–1000 cm⁻¹). Taking into account the close packing of the chromophores in the chlorosome, the difference is more likely to be much higher due to the narrowing effect. Another source of broadening could be the coupling of excitonic states to charge transfer (CT) states, which are expected to occur due to the close packing of the chromophores, and which were observed in Stark spectroscopy of chlorosomes.⁴⁵ However, the charge transfer from one neutral molecule to another is not energetically favorable unless the environment or external field (as in Stark spectroscopy) creates a potential that favors it. CT states can therefore be assumed to be sufficiently off resonance not to contribute in our experiment. Even if the environment did allow the CT states to have lower energy, the additional broadening due to resonance interaction of CT states with excitonic states cannot account for the very broad chlorosome absorption band.

Thus, we demonstrated that the upper estimate of the excitonic transition line width is much smaller than the diagonal line width of the observed 2D spectra. Consequently, the short time dynamics of the 2D spectrum do not reflect homogeneous line shape dynamics caused by the bath reorganization, but rather reveal excitation dynamics.

Effective Excitation Diffusion Model. As discussed above, the experimental spectra in Figure 2 reflect a significant inhomogeneous disorder in the chlorosomes and fast redistribution of transition energies on a sub-100 fs time scale. This behavior is reminiscent of spectral changes induced in a two-level system by pure dephasing due to interaction with a bath. The following analogy explores this possibility: the first excited-state manifold of a chlorosome will be considered as “one state”, a superlevel, which interacts with a “bath” of electronic levels of this manifold. These electronic levels can be then included into the model by an effective energy gap correlation function, analogously to the way the bath density of states is included for a two-level system. Because of the size and the high disorder of the chlorosome, the appropriate energy gap correlation function is expected to take a relatively simple form. First, at $t_2 = 0$ fs, the correlation function has to have a value consistent with the chlorosome absorption spectrum, that is, $C(0) = \Delta^2$. Second, random hopping among the coherent

domains corresponding to spectral and spatial diffusion of the excitation would lead to an exponential decay of the correlation. One could in principle expect some more complicated contribution from a possible coherent component of the energy transfer within the coherent domains at short times, but as there are many possible substructures with similar energies, any oscillatory signal due to electronic coherences will dephase because of ensemble averaging. It is important to note that the rephasing capability of photon echo does not apply to coherences within the electronic bands. This is due the fact that the third-order spectroscopic signal involves only one time interval (so-called population time) when these coherences evolve, and not two that could lead to rephasing. To properly describe the results of ultrafast chlorosome spectroscopy, it is necessary to include consideration of the two-exciton band, which appears in the 2D and pump–probe spectra as a source of excited state absorption. This will be done by the same effective superlevel method. To calculate 2D spectra of such an effective three level system, it is necessary to know the energy gap correlation functions $C_{ee}(t)$, $C_{ff}(t)$, and $C_{ef}(t)$, where $C_{ij}(t) = \langle \delta\omega_i(t)\delta\omega_j(0) \rangle$, and the $\delta\omega_i$ is the energy gap operator of the transition between the ground state and the superlevel *i*. Indices e and f denote the single- and two-exciton states. The correlation function is defined as

$$C_{ij}(t) = \gamma_{ij}\Delta^2 e^{-t/\tau_c} \quad (2)$$

that leads to a real line shape function of the form:

$$g_{ij}(t) = \gamma_{ij}\Delta^2 \tau_c^2 \left(e^{-t/\tau_c} + \frac{t}{\tau_c} - 1 \right) \quad (3)$$

where γ_{ij} ($\gamma_{ee} = 1$) is a prefactor, which adjusts the cross-correlation function $C_{ef}(t)$ and two-exciton correlation function $C_{ff}(t)$ relative to $C_{ee}(t)$. The same correlation time τ_c is set for all of them for simplicity. Thus, there are the following adjustable phenomenological parameters in the model: Δ , τ_c , and γ_{ij} , which are obtained by fitting simulated spectra to experimental results. Their effect on the shape of simulated 2D spectra is the following: Δ and τ_c are responsible for the overall shape and size of the 2D spectrum. In addition, τ_c provides the typical time scale of the dynamics. Parameter γ_{ff} adjusts the relative width in the diagonal and antidiagonal directions of the excited-state absorption signal, and γ_{ef} adjusts the excited-state signal shape deviation from the antidiagonal orientation.

Comparison between Simulation and Experiment. All simulations were done in the impulsive approximation, neglecting finite temporal and spectral width of the laser pulses. Values of the parameters needed to model the experimental data are summarized in Table 1. The energy gap between the ground and first excited superlevels ΔE_{ge} corresponding to 745 nm

Table 1. Values of the Parameters Used To Model the Experimental Data

ΔE_{ge} (eV)	ΔE_{ef} (eV)	μ_{ge} (au)	μ_{ef} (au)	τ_c (fs)	Δ^2 (rad ² fs ⁻²)	γ_{ee}	γ_{ff}	γ_{ef}
1.666	1.684	1	1.3	100	3.5×10^{-3}	1	4.3	1.8

dictates the position of the absorption band as well as the position of the positive signal in the 2D spectrum. The gap between the first and second excited superlevels ΔE_{ef} is set to be slightly larger than ΔE_{ge} to reproduce negative excited-state absorption signal that is more pronounced at higher energy part of the 2D and

transient absorption spectra. In the excitonic picture of the chlorosome, these energy gaps correspond to the relative energies of the strongly allowed single and double exciton bands. The values of the line shape parameter Δ , and correlation time τ_c are chosen to correctly reproduce the elongated shape of the 2D spectrum at $t_2 = 0$ fs. In addition, the correlation time of 100 fs governs the characteristic time scale of spectral dynamics. However, the exact time evolution of the particular areas of the 2D spectrum is given by interplay between decays of positive and negative contributions. The value of transition dipole moment μ_{ef} was set larger than μ_{ge} to adequately reproduce the experimental data. The shape of the negative signal is determined by the parameters γ_{ff} and γ_{ef} . Because γ_{ff} is bigger than γ_{ee} , which is set to 1, the negative signal is broader than the positive. The parameter γ_{ef} is adjusted to provide the correct negative signal inclination toward the diagonal direction.

Results of the simulation are compared to the experimental data in Figures 1–4. The simulated spectra were normalized in such a way that the maximum amplitudes of both the simulated and the experimental 2D spectra are equal at $t_2 = 0$ fs. It can be seen that the proposed simple model reproduces well the absorption spectrum (Figure 1), as well as the general shape and evolution of the 2D spectrum (Figure 2) with its characteristic maximal intensity drop (Figure 3). The noticeable difference in the modeled and observed absorption spectra comes from limitations of the model, whose parameters were optimized to preferentially reproduce the 2D spectra. Overall success of the model confirm that observed sub-100 fs dynamics comes from stochastic exciton diffusion. However, the model does not provide an interpretation of some detailed spectral features. The differences between the model and experimentally observed dynamics discussed below will be used to make further conclusions about the nature of the excitation dynamics.

First, the discrepancies between the experimental and simulated data are listed. In particular, the slope of the nodal line separating positive and negative parts changes little during the time evolution in the experimental data. In the simulation, however, it leans from diagonal direction at $t_2 = 0$ fs to an almost horizontal orientation at $t_2 = 200$ fs. The difference is also observed in the ω_1 -integrated profiles corresponding to the transient absorption signal. The general shape is similar at $t_2 = 0$ fs; only the maximum of the simulated spectrum is blue-shifted by 5 nm. The projection of the experimental spectrum at later times decays and shifts to the red side, whereas the simulated projection remains without any change.

In the following, the insight provided by the diffusion model and its limitations is combined with the coherent domain structural model to interpret the initial excitation dynamics in the chlorosome. The effective excitation diffusion model describes the chlorosome as a set of coherent domains between which random energy transfer is taking place. When energy starts diffusing between the domains in an incoherent manner, all coherence dynamics effects (if initiated by the initial excitation) are quickly dephased. Positive signal at the time immediately after excitation correlates excitation and detection frequencies from the transitions in the same coherent domain. Individual coherent domains are weakly coupled, which prevents formation of observable cross-peaks between different domains. Nevertheless, the energy transfer between the domains is very fast, because of the presence of a multitude of exciton transitions with similar energy, but likely with different oscillator strength. Strongly elongated shape at $t_2 = 0$

fs is the result of a broad energetic distribution of coherent domains. The antidiagonal width of the positive band is given by the average properties of a single domain. In general, it cannot be simply identified with the homogeneous line width of a single exciton level because there can be several excitonic transitions localized in one coherent domain sharing a common ground state. Thus, the 2D spectrum of a single coherent domain is a superposition of diagonal- and cross-peaks. In agreement with the exciton theory, which predicts comparable spacing between bands, the whole positive signal is overlaid with a broad negative signal arising from single- to double-exciton absorption. The temporal evolution of the 2D spectrum reflects energy redistribution between neighboring domains. Because stochastic energy diffusion in the simulation is completely random, without any preferred direction, the positive signal of the 2D spectrum acquires a rounded shape with a horizontal nodal line, and the red-shift dynamics in the integrated projection is not observed. The model does not take into account any oscillator strength differences between transitions belonging to different coherent domains. This prevents the decay of the transient signal and, together with the effect described above, leads to the complete lack of time evolution in the integrated projection (Figure 4). However, in the chlorosome, we observe energy diffusion in which coherent domains with allowed exciton transitions at higher energies populate similar and lower energy exciton transitions located in the neighboring domains. This downhill process results in a filling of the space under the diagonal by a positive signal. Because some high energy domains remain excited during the diffusion process, the direction of nodal line remains almost unchanged. The fact that after 200 fs the low energy side of the positive signal is not completely horizontal indicates that the excitation energy redistribution is not completed on this time scale. The preferred downhill direction can be also observed as a red shift of a transient absorption signal (Figure 4). The intensity drop of the integrated projection is explained by the fact that levels with a strong transition dipole moment are initially excited, but levels with a weaker dipole moment become populated during the energy redistribution within and between coherent domains. This observation supports the previously reported suggestion that the lowest excitonic states in the chlorosome aggregates possess small transition dipole moments.^{19,26,37} Similar initial energy transfer dynamics were observed in chlorosomes from *Chloroflexus aurantiacus* as well (see the Supporting Information), indicating that this form of ultrafast energy migration is a general phenomenon in chlorosomes.

Note that the ensemble average of a broad range of dynamical processes taking place in photoexcited chlorosomes was observed. For example, the energy of the photons absorbed very close to the baseplate will be immediately transferred to the baseplate without initial energy diffusion. However, these instances are rare and do not contribute substantially to the observed signal. By observing the average excitation energy dynamics in this work, the most common and most important initial processes of the chlorosome light-harvesting function were investigated.

CONCLUSIONS

We report a study of initial excitation evolution in chlorosomes on a sub-100 fs time scale that has not been explored previously. Excitation dynamics monitored as spectral changes in the 2D spectra are explained by proposing a model of

effective diffusion-like behavior of the excitons. Following initial excitation, energy diffuses extremely fast among and within coherent domains of the chlorosome. Most of the inhomogeneous transition energy distribution in the chlorosome is sampled by the spectral diffusion within 200 fs. The presence of a coherent energy transfer component within the chlorosome substructures on an even shorter time scale cannot be excluded, because oscillatory contributions to the 2D spectrum are likely to be smeared out by the significant static disorder within chlorosomes. According to the proposed model, energy diffusion causes rapid dephasing between the coherent domains, and thus the electronic phase relationship between the domains is lost. This implies that the overall energy transfer through the chlorosome as a light-harvesting unit cannot proceed coherently.

MATERIALS AND METHODS

Cells of *Cba. tepidum* were grown as described previously,⁹ and the chlorosomes were isolated following a standard method consisting of two successive sucrose gradient ultracentrifugation steps.⁴⁶ Before the measurement, chlorosomes were dissolved in 50 mM Tris-HCl buffer (pH 8.0), sucrose was removed using a centrifugal filter, and the sample was diluted to absorbance of about 0.4 in a 0.5 mm optical path at 745 nm. In addition, chlorosomes were reduced by 15 mM sodium dithionite and incubated at least 45 min before measurement to achieve anaerobic conditions. All experiments were carried out in a 0.5 mm optical path length flow cell. The sample was flowed at ~10 cm/s rate. Excitation intensity was typically 100 pJ per pulse in each of excitation pulse, which corresponds to approximately 4.8×10^{12} photons per pulse per cm² that satisfies annihilation-free conditions.¹⁹

2D spectra were obtained using the double-modulation lock-in technique described in ref 47. Briefly, a 200 kHz repetition rate KGW amplified laser system (PHAROS, Light Conversion) was used to pump a homemade NOPA that produced broadband 15 fs pulses centered at 750 nm with spectral fwhm of ~95 nm. Using a plate beam splitter and transmissive diffraction grating, the initial beam is split into four beams arranged in the boxcar geometry. One of them, the local oscillator (LO) beam is attenuated by a 3 OD filter. The other three beams are used to excite the sample in a four wave mixing experiment. The first and second beams are modulated at different frequencies, using optical choppers. Accurate time delays of the first two pulses are introduced by moving fused silica wedges with motorized translation stages. Polarization induced in the sample is emitted in the phase-matched direction, mixed with the collinear LO beam, and detected in a spectral interferometry scheme. Detection of the third-order signal is performed by locking to the sum and difference of the chopper modulation frequencies.

ASSOCIATED CONTENT

Supporting Information

2D spectra of chlorosomes from *Chloroflexus aurantiacus*. This material is available free of charge via the Internet at <http://pubs.acs.org>.

AUTHOR INFORMATION

Corresponding Author

donatas.zigmantas@chemphys.lu.se

Present Address

[†]Center for Physical Sciences and Technology, Gostauto 11, LT-01108 Vilnius, Lithuania.

Notes

The authors declare no competing financial interest.

ACKNOWLEDGMENTS

We would like to thank A. M. Collins and R. E. Blankenship from Washington University in St. Louis for providing *Cfl. aurantiacus*

chlorosome samples and Wilfred Fullagar for critically reading the manuscript. The work in Lund was supported by the Swedish Research Council, the Knut and Alice Wallenberg Foundation, Wenner-Gren Foundations, and LASERLAB-EUROPE. The work in Prague was supported by the Grant Agency of Charles University (GAUK 129809), Czech Ministry of Education, Youth and Sports (project MSM0021620835), and Czech Science Foundation (project 206/09/0375).

REFERENCES

- (1) Frigaard, N.-U.; Bryant, D. In *Complex Intracellular Structures in Prokaryotes*; Shively, J., Ed.; Springer: Berlin/Heidelberg, 2006; Vol. 2, p 79.
- (2) Bryant, D. A.; Costas, A. M. G.; Maresca, J. A.; Chew, A. G. M.; Klett, C. G.; Bateson, M. M.; Tallon, L. J.; Hostetler, J.; Nelson, W. C.; Heidelberger, J. F.; Ward, D. M. *Science* **2007**, *317*, 523.
- (3) Blankenship, R. E.; Matsuura, K. In *Light-Harvesting Antennas in Photosynthesis*; Green, B. R., Parson, W. W., Eds.; Kluwer Academic Publishers: Dordrecht, 2003; p 195.
- (4) Katterle, M.; Prokhorenko, V. I.; Holzwarth, A. R.; Jesorka, A. *Chem. Phys. Lett.* **2007**, *447*, 284.
- (5) Roger, C.; Miloslavina, Y.; Brunner, D.; Holzwarth, A. R.; Wurthner, F. *J. Am. Chem. Soc.* **2008**, *130*, 5929.
- (6) Huijser, A.; Marek, P. L.; Savenije, T. J.; Siebbeles, L. D. A.; Scherer, T.; Hauschild, R.; Szmytkowski, J.; Kalt, H.; Hahn, H.; Balaban, T. S. *J. Phys. Chem. C* **2007**, *111*, 11726.
- (7) Miyatake, T.; Tamiaki, H. *Coord. Chem. Rev.* **2010**, *254*, 2593.
- (8) Alster, J.; Polivka, T.; Arellano, J. B.; Chabera, P.; Vacha, F.; Psencik, J. *Chem. Phys.* **2010**, *373*, 90.
- (9) Psencik, J.; Ikonen, T. P.; Laurinmaki, P.; Merckel, M. C.; Butcher, S. J.; Serimaa, R. E.; Tuma, R. *Biophys. J.* **2004**, *87*, 1165.
- (10) Oostergetel, G. T.; Reus, M.; Chew, A. G. M.; Bryant, D. A.; Boekema, E. J.; Holzwarth, A. R. *FEBS Lett.* **2007**, *581*, 5435.
- (11) Psencik, J.; Torkkeli, M.; Zupcanova, A.; Vacha, F.; Serimaa, R. E.; Tuma, R. *Photosynth. Res.* **2010**, *104*, 211.
- (12) Oostergetel, G. T.; van Amerongen, H.; Boekema, E. J. *Photosynth. Res.* **2010**, *104*, 245.
- (13) Holzwarth, A. R.; Schaffner, K. *Photosynth. Res.* **1994**, *41*, 225.
- (14) Nozawa, T.; Ohtomo, K.; Suzuki, M.; Nakagawa, H.; Shikama, Y.; Konami, H.; Wang, Z. Y. *Photosynth. Res.* **1994**, *41*, 211.
- (15) Egawa, A.; Fujiwara, T.; Mizoguchi, T.; Kakitani, Y.; Koyama, Y.; Akutsu, H. *Proc. Natl. Acad. Sci. U.S.A.* **2007**, *104*, 790.
- (16) Ganapathy, S.; Oostergetel, G. T.; Wawrzyniak, P. K.; Reus, M.; Gomez Maqueo Chew, A.; Buda, F.; Boekema, E. J.; Bryant, D. A.; Holzwarth, A. R.; de Groot, H. J. *Proc. Natl. Acad. Sci. U.S.A.* **2009**, *106*, 8525.
- (17) Jochum, T.; Reddy, C. M.; Eichhofer, A.; Buth, G.; Szmytkowski, J.; Kalt, H.; Moss, D.; Balaban, T. S. *Proc. Natl. Acad. Sci. U.S.A.* **2008**, *105*, 12736.
- (18) Savikhin, S.; Zhu, Y. W.; Blankenship, R. E.; Struve, W. S. *J. Phys. Chem.* **1996**, *100*, 17978.
- (19) Psencik, J.; Ma, Y. Z.; Arellano, J. B.; Hala, J.; Gillbro, T. *Biophys. J.* **2003**, *84*, 1161.
- (20) Martiskainen, J.; Linnanto, J.; Kananavicius, R.; Lehtovuori, V.; Korppi-Tommola, J. *Chem. Phys. Lett.* **2009**, *477*, 216.
- (21) Causgrove, T. P.; Brune, D. C.; Blankenship, R. E. *J. Photochem. Photobiol. B* **1992**, *15*, 171.
- (22) Savikhin, S.; Zhu, Y. W.; Lin, S.; Blankenship, R. E.; Struve, W. S. *J. Phys. Chem.* **1994**, *98*, 10322.
- (23) Savikhin, S.; Vannoort, P. I.; Blankenship, R. E.; Struve, W. S. *Biophys. J.* **1995**, *69*, 1100.
- (24) Savikhin, S.; Vannoort, P. I.; Zhu, Y. W.; Lin, S.; Blankenship, R. E.; Struve, W. S. *Chem. Phys.* **1995**, *194*, 245.
- (25) Ma, Y. Z.; Aschenbrucker, J.; Miller, M.; Gillbro, T. *Chem. Phys. Lett.* **1999**, *300*, 465.
- (26) Prokhorenko, V. I.; Steensgaard, D. B.; Holzwarth, A. R. *Biophys. J.* **2000**, *79*, 2105.
- (27) Jonas, D. M. *Annu. Rev. Phys. Chem.* **2003**, *54*, 425.

- (28) Engel, G. S.; Calhoun, T. R.; Read, E. L.; Ahn, T. K.; Mancal, T.; Cheng, Y. C.; Blankenship, R. E.; Fleming, G. R. *Nature* **2007**, *446*, 782.
- (29) Collini, E.; Wong, C. Y.; Wilk, K. E.; Curmi, P. M.; Brumer, P.; Scholes, G. D. *Nature* **2010**, *463*, 644.
- (30) Mancal, T.; Nemeth, A.; Milota, F.; Lukes, V.; Kauffmann, H. F.; Sperling, J. *J. Chem. Phys.* **2010**, *132*, 184515.
- (31) Nemeth, A.; Milota, F.; Mancal, T.; Lukes, V.; Hauer, J.; Kauffmann, H. F.; Sperling, J. *J. Chem. Phys.* **2010**, *132*, 184514.
- (32) Nemeth, A.; Milota, F.; Mancal, T.; Lukes, V.; Kauffmann, H. F.; Sperling, J. *Chem. Phys. Lett.* **2008**, *459*, 94.
- (33) Sumi, H. *J. Phys. Chem. B* **1999**, *103*, 252.
- (34) Scholes, G. D.; Fleming, G. R. *J. Phys. Chem. B* **2000**, *104*, 1854.
- (35) Zigmantas, D.; Read, E. L.; Mancal, T.; Brixner, T.; Gardiner, A. T.; Cogdell, R. J.; Fleming, G. R. *Proc. Natl. Acad. Sci. U.S.A.* **2006**, *103*, 12672.
- (36) Fetisova, Z. G.; Mauring, K.; Taisova, A. S. *Photosynth. Res.* **1994**, *41*, 205.
- (37) Psencik, J.; Polivka, T.; Nemec, P.; Dian, J.; Kudrna, J.; Maly, P.; Hala, J. *J. Phys. Chem. A* **1998**, *102*, 4392.
- (38) Saga, Y.; Wazawa, T.; Mizoguchi, T.; Ishii, Y.; Yanagida, T.; Tamiaki, H. *Photochem. Photobiol.* **2002**, *75*, 433.
- (39) Furumaki, S.; Vacha, F.; Habuchi, S.; Tsukatani, Y.; Bryant, D. A.; Vacha, M. *J. Am. Chem. Soc.* **2011**, *133*, 6703.
- (40) Saga, Y.; Shibata, Y.; Tamiaki, H. *J. Photochem. Photobiol., C* **2010**, *11*, 15.
- (41) Tian, Y.; Camacho, R.; Thomsson, D.; Reus, M.; Holzwarth, A. R.; Scheblykin, I. G. *J. Am. Chem. Soc.* **2011**, *133*, 17192.
- (42) Mukamel, S. *Principles of Nonlinear Optical Spectroscopy*; Oxford University Press: New York, 1995.
- (43) Cho, M. H.; Yu, J. Y.; Joo, T. H.; Nagasawa, Y.; Passino, S. A.; Fleming, G. R. *J. Phys. Chem.* **1996**, *100*, 11944.
- (44) Brune, D. C.; Blankenship, R. E.; Seely, G. R. *Photochem. Photobiol.* **1988**, *47*, 759.
- (45) Frese, R.; Oberheide, U.; van Stokkum, I.; van Grondelle, R.; Foidl, M.; Oelze, J.; van Amerongen, H. *Photosynth. Res.* **1997**, *54*, 115.
- (46) Steensgaard, D. B.; Matsuura, K.; Cox, R. P.; Miller, M. *Photochem. Photobiol.* **1997**, *65*, 129.
- (47) Augulis, R.; Zigmantas, D. *Opt. Express* **2011**, *19*, 13126.

■ NOTE ADDED AFTER ASAP PUBLICATION

Table 1 contained an error in the version published ASAP July 2, 2012. The heading in column 3 was corrected and this paper reposted on July 5, 2012.